NASA Technical Paper 1887

An Application of Multivariable Design Techniques to the Control of the National Transonic Facility

Ernest S. Armstrong and John S. Tripp

AUGUST 1981

NASA

NASA Technical Paper 1887

An Application of Multivariable Design Techniques to the Control of the National Transonic Facility

Ernest S. Armstrong and John S. Tripp
Langley Research Center
Hampton, Virginia

SUMMARY

The digital versions of optimal-linear-regulator theory and eigenvalue placement theory are applied to the Mach number control loop of the National Transonic Facility cryogenic wind tunnel. The control laws developed are evaluated on a nonlinear simulation of the tunnel process for a typical test condition and are found to significantly reduce the open-loop time required to achieve a Mach number set point.

INTRODUCTION

The National Transonic Facility (NTF), figure 1, will be a continuous-flow cryogenic wind tunnel designed to satisfy the basic airfoil research and development needs of the federal government and industry. The tunnel (refs. 1 and 2) will operate on the basic principle that Reynolds number is inversely proportional to temperature. It is expected to achieve an order of magnitude increase in Reynolds number over existing tunnels at reasonable values of dynamic pressure by injecting liquid nitrogen as a coolant to maintain the test gas at cryogenic temperatures. The NTF will be controlled by a digital computer in order to achieve high productivity and to implement control of dynamic pressure, Mach number, and Reynolds number, or other equivalent sets of process variables.

A plan view of the tunnel control circuit is shown in figure 2. The NTF will be a closed-circuit fan-driven pressure tunnel capable of total pressures up to 896 318 Pa (130 psi). It will have a 6.25-m^2 (67.24-ft^2) slotted test section which will be 61 m (200 ft) long and 14.6 m (48 ft) wide. It will operate from room temperature to 88.70 K (-300°F). Liquid nitrogen (LN_2) will be sprayed into the circuit upstream of the fan (a) for the initial cooldown phase, (b) to balance the heat rise associated with the gas compression by the fan, (c) during steady-state temperature regulation, and (d) to act as the primary mode of temperature control in the test section. During the ambient temperature operation (air mode) of the NTF cooling functions, (b), (c), and (d) are taken over by a heat exchanger, located in the stagnation section, and an external cooling tower. No LN_2 is consumed in the air mode. Pressure control is provided by venting gaseous nitrogen (GN_2) from the tunnel to the outdoors. Coarse Mach number control will be provided by fan motor speed regulation, and fine vernier Mach number variations will be controlled with small changes about a constant reference guide vane angle.

Digital computers and microprocessors will be employed for automation and process control of the NTF. Among the functions planned for computer operation are supervisory set-point programming, monitoring process limits, sequencing and timing, and automation of the start-up and shutdown operational sequence. Additionally, the digital capability will offer the opportunity to apply multivariable control techniques to the wind-tunnel process. The purpose of this report is to demonstrate the use of two multivariable methods to design control laws for a particular NTF operating condition.

Analytical studies of the NTF process have produced a transfer function describing, in the s-domain, the dominant interaction of the test-section Mach number and fan guide vane angle when the process is perturbed from a steady-state operating condition. This transfer function is employed herein to demonstrate the application of multivariable design methods to the Mach number control loop of the NTF. Initially, in order to overcome a design difficulty presented by a transport lag appearing in the transfer function and to generate time-domain equations needed for multivariable design, finite-difference equations are derived which approximate the Mach number to guide vane angle characteristics for zero-order hold guide vane actuator and actuator rate inputs. Optimal linear regulator and eigenvalue placement techniques (refs. 3 and 4) are next applied to derive multivariable feedback control laws for Mach number regulation about a typical steady-state operating condition. System responses are calculated from the linear finite-difference design equations and a nonlinear simulation, which solves the Navier-Stokes partial differential equations for unsteady flow to represent the fluid flow dynamics.

SYMBOLS and ABBREVIATIONS

A   response matrix for state equation in variable x (see eqs. (A4), (31), and (34))

A_0, A_1 defined by equations (15) and (16)

$\hat{A}_0, \hat{A}_1, \hat{A}_2$ defined by equations (20), (21), and (22)

B   control effectiveness matrix for state equation in variable x (see eqs. (A4), (32), and (35))

B_0 defined by equation (17)

B_1 defined by equation (A1)

$\hat{B}_0$ defined by equation (23)

$\hat{B}_1$ defined by equation (A13)

col   column matrix

diag   diagonal matrix

f   feedback gain

GN_2 gaseous nitrogen

h   time delay, sec

i   nonnegative integer

j $= \sqrt{-1}$

2

k	gain in transfer function defined by equation (1), $\deg^{-1}$
LN_2	liquid nitrogen
M	Mach number
M_f	set-point Mach number
m	natural number defined by equation (18)
N	positive integer, such that $N\Delta = T$
P	defined by equation (45)
$P_{t,f}$	set-point total pressure, Pa
Q	weighting matrix in equation (45)
rpm	revolutions per minute
s	Laplace transform parameter
T	final time for matrix equation (A1), sec
$T_{t,f}$	set-point total temperature, K
t	time, sec
t_s	settling time, sec
u	control variable
x	state vector defined by equations (33) and (36)
$\tilde{x}$	state vector defined by equation (14)
z	defined by equation (24)
Δ	sampling period, sec
δM	Mach number perturbation
$\delta\theta$	guide vane angle perturbation
$\delta\theta_A$	guide vane angle actuator-input perturbation
ζ	damping ratio
θ	guide vane angle, deg
θ_A	guide vane angle actuator input

θ_f set-point guide vane angle, deg

τ time constant, sec

ϕ matrix defined by equation (46)

ω frequency, rad/sec

$t \in \lceil a,b)$ $a \leqq t < b$

$\approx$ approximately equal

A dot over a symbol denotes differentiation with respect to time.

A prime after a symbol denotes a matrix transpose.

MACH NUMBER TRANSFER FUNCTION CHARACTERISTICS

This section describes some basic characteristics of the NTF Mach number control loop. The information to be presented was obtained by means of private communication from George Gumas, Pennsylvania State University, Middletown, Pennsylvania.

Consider the NTF process to be operating in a steady-state condition such that, for some fixed fan speed, constant values of guide vane angle, liquid-nitrogen injection rate, and gaseous-nitrogen vent rate are chosen to maintain all tunnel states at zero time rate of change. When the guide vane angle is perturbed from its steady-state value, while maintaining the liquid-nitrogen injection and gaseous-nitrogen vent rates, the transfer function between test-section Mach number and fan guide vane angle closely approximates the following equation if no acoustic modes are excited and perturbations remain small:

$$\frac{\delta M(s)}{\delta \theta(s)} = \frac{ke^{-hs}}{(\tau s + 1)} \tag{1}$$

The symbols $\delta M(s)$ and $\delta \theta(s)$ represent, in the s-domain, the perturbations away from steady-state Mach number M_f and guide vane angle θ_f and are given as

$$\delta M(s) = M(s) - M_f/s \tag{2}$$

and

$$\delta \theta(s) = \theta(s) - \theta_f/s \tag{3}$$

4

The constants k and τ in equation (1) depend parametrically on the operating condition. Tables I to III (provided by George Gumas) show k and τ values for steady-state test-section total temperature $T_{t,f}$ and Mach number M_f. The transport lag h is approximated by

$$h = 4.29/\sqrt{T_{t,f}} \qquad (4)$$

Additionally, the guide vane angle is set through an actuator with the transfer function approximated by

$$\frac{\delta\theta(s)}{\delta\theta_A(s)} = \omega^2/(s^2 + 2\zeta\omega s + \omega^2) \qquad (5)$$

where

$$\omega = 6.0 \text{ rad/sec}$$

and

$$\zeta = 0.8$$

and where

$$\delta\theta_A(s) = \theta_A(s) - \theta_f/s \qquad (6)$$

and θ_A is the transient value of the input to the guide vane actuator.

Operational constraints limit the values of guide vane angle θ and guide vane angle rate $\dot{\theta}$ to lie within $\pm30^\circ$ and $\pm30^\circ$/sec, respectively.

Control laws are derived for $\delta\theta_A$ and $\delta\dot{\theta}_A$ which regulate the Mach number about the steady-state value M_f. Block diagrams for the composite transfer-function sequences are shown in figure 3. The multivariable design methods to be applied require constant-coefficient time-domain equations for equations (1) and (5) which are developed in the section which follows.

5

MATHEMATICAL MODELS FOR MULTIVARIABLE CONTROL DESIGN

In this section, time-domain vector-matrix equations of the form

$$x[(i + 1)\Delta] = A\ x(i\Delta) + B\ u(i\Delta) \qquad (i = 0,1,\ldots) \qquad (7)$$

are developed from the dynamics of the test-section Mach number expressed in the s-domain by equations (1) and (5). The matrices A and B in equation (7) are constant and Δ is the sampling period for applying either of the zero-order hold controls:

guide vane actuator input

$$u(i\Delta) = \delta\theta_A(i\Delta) \qquad (8)$$

or guide vane actuator rate input

$$u(i\Delta) = \delta\dot{\theta}_A(i\Delta) \qquad (9)$$

The Mach number response $\delta M(i\Delta)$ is one of the elements of the state vector x.

The delay equation

$$\tau\ \delta\dot{M}(t) + \delta M(t) = k\ \delta\theta(t - h) \qquad (10)$$

and the ordinary differential equation

$$\delta\ddot{\theta}(t) + 2\zeta\omega\ \delta\dot{\theta}(t) + \omega^2\ \delta\theta(t) = \omega^2\ \delta\theta_A(t) \qquad (11)$$

have the same input-output characteristics as equations (1) and (5), respectively. Equations (10) and (11) can be written in state-variable form as

$$\dot{\tilde{x}}(t) = A_0\ \tilde{x}(t) + A_1\ \tilde{x}(t - h) + B_0\ u(t) \qquad (12)$$

where

$$u(t) = \delta\theta_A(t) \qquad (13)$$

$$\tilde{x}(t) = \begin{bmatrix} \tilde{x}_1(t) \\ \tilde{x}_2(t) \\ \tilde{x}_3(t) \end{bmatrix} = \begin{bmatrix} \delta M(t) \\ \delta \theta(t) \\ \delta \dot{\theta}(t) \end{bmatrix} \qquad (14)$$

$$A_0 = \begin{bmatrix} -1/\tau & 0 & 0 \\ 0 & 0 & 1 \\ 0 & -\omega^2 & -2\zeta\omega \end{bmatrix} \qquad (15)$$

$$A_1 = \begin{bmatrix} 0 & k/\tau & 0 \\ 0 & 0 & 0 \\ 0 & 0 & 0 \end{bmatrix} \qquad (16)$$

and

$$B_0 = \begin{bmatrix} 0 \\ 0 \\ \omega2 \end{bmatrix} \qquad (17)$$

Multivariable techniques exist which could be applied directly to equation (12), but the calculations are greatly complicated by the presence of the time delay h. One approach to overcoming the problem of time delays is to use a zero-order hold structure for the control and approximate the time delay by an integral multiple of the sampling period; that is,

$$m\Delta \approx h \qquad (18)$$

for some nonnegative integer m.

This approach to treating time delays is described in the appendix and, when applied to equation (12), produces

$$\tilde{x}[(i+1)\Delta] = \hat{A}_0 \, \tilde{x}(i\Delta) + \hat{A}_1 \, \tilde{x}[(i-m)\Delta] + \hat{A}_2 \, \tilde{x}[(i-m+1)\Delta] + \hat{B}_0 \, u(i\Delta) \qquad (19)$$

7

where

$$\hat{A}_0 = e^{A_0\Delta} = \begin{bmatrix} e^{-\Delta/\tau} & 0 & 0 \\ 0 & e^{-\zeta\Delta\omega}\cos\left(\Delta\omega\sqrt{1-\zeta^2}\right) + \left(\zeta/\sqrt{1-\zeta^2}\right)e^{-\zeta\Delta\omega}\sin\left(\Delta\omega\sqrt{1-\zeta^2}\right) & \left(1/\omega\sqrt{1-\zeta^2}\right)e^{-\zeta\Delta\omega}\sin\left(\Delta\omega\sqrt{1-\zeta^2}\right) \\ 0 & \left(-\omega/\sqrt{1-\zeta^2}\right)e^{-\zeta\Delta\omega}\sin\left(\Delta\omega\sqrt{1-\zeta^2}\right) & e^{-\zeta\Delta\omega}\cos\left(\Delta\omega\sqrt{1-\zeta^2}\right) - \left(\zeta/\sqrt{1-\zeta^2}\right)e^{-\zeta\Delta\omega}\sin\left(\Delta\omega\sqrt{1-\zeta^2}\right) \end{bmatrix}$$

(20)

$$\hat{A}_1 = \frac{\Delta}{2}e^{A_0\Delta}A_1 = \begin{bmatrix} 0 & \dfrac{\Delta k}{2\tau}e^{-\Delta/\tau} & 0 \\ 0 & 0 & 0 \\ 0 & 0 & 0 \end{bmatrix}$$

(21)

$$\hat{A}_2 = \frac{\Delta}{2}A_1 = \begin{bmatrix} 0 & \dfrac{\Delta k}{2\tau} & 0 \\ 0 & 0 & 0 \\ 0 & 0 & 0 \end{bmatrix}$$

(22)

and

$$\hat{B}_0 = \int_0^\Delta e^{A_0\tau}\,d\tau\, B_0$$

(23)

Because of the sparseness of $\hat{A}_1$ and $\hat{A}_2$, the delayed terms in equation (19) involve only the variable $\tilde{x}_2$. After introducing m (eq. (18)) additional variables and equations of the form

$$\left. \begin{aligned} z_1[(i+1)\Delta] &= \tilde{x}_2[(i-m+1)\Delta] = z_2(i\Delta) \\ z_2[(i+1)\Delta] &= \tilde{x}_2[(i-m+2)\Delta] = z_3(i\Delta) \\ &\quad\vdots \\ z_{m-1}[(i+1)\Delta] &= \tilde{x}_2[(i-1)\Delta] = z_m(i\Delta) \\ z_m[(i+1)\Delta] &= \tilde{x}_2(i\Delta) \end{aligned} \right\}$$

(24)

then equations (19) to (24) can be combined to construct an equation of the form of equation (7) with state vector

$$x(i\Delta) = \begin{bmatrix} \tilde{x}_1(i\Delta) \\ \tilde{x}_2(i\Delta) \\ \tilde{x}_3(i\Delta) \\ z_1(i\Delta) \\ z_2(i\Delta) \\ \cdot \\ \cdot \\ \cdot \\ z_m(i\Delta) \end{bmatrix} = \begin{bmatrix} \delta M(i\Delta) \\ \delta\theta(i\Delta) \\ \delta\dot{\theta}(i\Delta) \\ \delta\theta[(i-m)\Delta] \\ \delta\theta[(i-m+1)\Delta] \\ \cdot \\ \cdot \\ \cdot \\ \delta\theta[(i-1)\Delta] \end{bmatrix} \qquad (25)$$

and guide vane actuator input control given by equation (8).

The coefficient matrices depend parametrically on the operating condition and sampling period chosen. A typical set of conditions for NTF operation within a linear region of the data sets of tables I to III was selected for this study. These conditions are as follows:

$$\left.\begin{array}{l} M_f = 0.9 \\ \\ T_{t,f} = 166.67 \text{ K } (-160^\circ\text{F}) \\ \\ P_{t,f} = 517\ 107 \text{ Pa } (75 \text{ psi}) \end{array}\right\} \qquad (26)$$

The fan is operated at synchronous speed. Table II lists

$$\left.\begin{array}{l} \tau = 1.964 \text{ sec} \\ \\ k = -0.0117 \text{ deg}^{-1} \end{array}\right\} \qquad (27)$$

and equation (4) yields

$$h = 0.33 \text{ sec} \qquad (28)$$

Then, for a sampling period of

$$\Delta = 0.1 \text{ sec} \tag{29}$$

the selection of

$$m = 4 \tag{30}$$

causes the actual value of $i\Delta + h$ to fall within the $[i\Delta - m\Delta, \quad i\Delta - (m - 1)\Delta]$ interval in equation (19). For the conditions shown in equations (26), the set-point guide vane angle θ_f is 1.93°. Using the foregoing numerical data and the guide vane actuator as the control $u(i\Delta)$, it can be determined that

$$A = \begin{bmatrix} 0.95035 & 0 & 0 & -0.002831 & -0.0002779 & 0 & 0 \\ 0 & 0.86976 & 0.06055 & 0 & 0 & 0 & 0 \\ 0 & -2.1798 & 0.28848 & 0 & 0 & 0 & 0 \\ 0 & 0 & 0 & 0 & 1 & 0 & 0 \\ 0 & 0 & 0 & 0 & 0 & 1 & 0 \\ 0 & 0 & 0 & 0 & 0 & 0 & 1 \\ 0 & 1 & 0 & 0 & 0 & 0 & 0 \end{bmatrix} \tag{31}$$

and

$$B = \begin{bmatrix} 0 \\ 0.1302 \\ 2.1798 \\ 0 \\ 0 \\ 0 \\ 0 \end{bmatrix} \tag{32}$$

with

10

$$x(i\Delta) = \begin{bmatrix} \delta M(i\Delta) \\ \delta\theta(i\Delta) \\ \delta\dot{\theta}(i\Delta) \\ \delta\theta[(i-4)\Delta] \\ \delta\theta[(i-3)\Delta] \\ \delta\theta[(i-2)\Delta] \\ \delta\theta[(i-1)\Delta] \end{bmatrix} \qquad (33)$$

Likewise, using guide vane actuator rate as the control $u(i\Delta)$, a similar procedure yields

$$A = \begin{bmatrix} 0.95035 & 0 & 0 & 0 & -0.0002831 & -0.0002979 & 0 & 0 \\ 0 & 0.86976 & 0.06055 & 0.1302 & 0 & 0 & 0 & 0 \\ 0 & -2.1798 & 0.28848 & 2.1798 & 0 & 0 & 0 & 0 \\ 0 & 0 & 0 & 1 & 0 & 0 & 0 & 0 \\ 0 & 0 & 0 & 0 & 0 & 1 & 0 & 0 \\ 0 & 0 & 0 & 0 & 0 & 0 & 1 & 0 \\ 0 & 0 & 0 & 0 & 0 & 0 & 0 & 1 \\ 0 & 1 & 0 & 0 & 0 & 0 & 0 & 0 \end{bmatrix}$$

$$(34)$$

and

$$B = \begin{bmatrix} 0 \\ 0.0047188 \\ 0.13024 \\ 0.1 \\ 0 \\ 0 \\ 0 \\ 0 \end{bmatrix} \qquad (35)$$

with

$$x(i\Delta) = \begin{bmatrix} \delta M(i\Delta) \\ \delta \theta(i\Delta) \\ \delta \dot{\theta}(i\Delta) \\ \delta \theta_A(i\Delta) \\ \delta \theta[(i-4)\Delta] \\ \delta \theta[(i-3)\Delta] \\ \delta \theta[(i-2)\Delta] \\ \delta \theta[(i-1)\Delta] \end{bmatrix}$$

(36)

Now that equations (1) and (5) have been combined to form equation (7), the multivariable design techniques are applied in the section which follows.

DESIGN AND LINEAR SIMULATION

Equation (7), with coefficients and state variables defined either by equations (31), (32), and (33), or (34), (35), and (36), represents variational equations linearized about the set point of equation (26). The design problem considered in this report is to assume that the system is initially perturbed from the operating point and derive, for either equation (8) or equation (9), constant-gain state-variable-feedback control laws which cause the Mach number and guide vane values to return rapidly to the operational set without violating the constraints

$$-30^\circ \leq \theta(t) \leq 30^\circ$$

(37)

and

$$-30^\circ/\text{sec} \leq \dot{\theta}(t) \leq 30^\circ/\text{sec}$$

(38)

In other words, control laws of the form

$$u(i\Delta) = -f' \, x(i\Delta)$$

(39)

are sought such that

12

$$\lim_{i \to \infty} x(i\Delta) \to 0 \tag{40}$$

without violating contraints (37) and (38) when

$$x[(i + 1)\Delta] = [A - Bf'] x(i\Delta) \tag{41}$$

and

$$x(0) \neq 0 \tag{42}$$

Two techniques, the optimal-linear-regulator and eigenvalue placement algorithms (refs. 3 and 4) are employed to form the control gains.

The optimal-linear-regulator algorithm finds the feedback gain by selecting the controller which minimizes a quadratic performance index

$$J = \sum_{i=0}^{\infty} \{x'[(i + 1)\Delta] \, Qx[(i + 1)\Delta] + u^2(i\Delta)\} \tag{43}$$

subject to equation (7), where Q is a nonnegative-definite symmetric weighting matrix. When certain controllability conditions (ref. 4) are satisfied, the gain is given by

$$f' = (1 + B'PB)^{-1}B'PA \tag{44}$$

with

$$P = \phi'P\phi + ff' + Q \tag{45}$$

and

$$\phi = A - Bf' \tag{46}$$

Software for solving equations (44), (45), and (46) is described in reference 3. Parametric studies of the elements of Q provided the choice of

$$Q = \text{diag} \, (10^4, 0, \ldots, 0)$$

13

as a weighting matrix yielding control gains which, upon simulation, typically produced responses satisfying the constraints $-30° \leq \theta(t) \leq 30°$ and $-30°/\text{sec} \leq \dot{\theta}(t) \leq 30°/\text{sec}$. For A, B, and x as given in equations (31), (32), and (33), the optimal regulator procedure gave the control law

$$\delta\theta_A(i\Delta) = 31.73\ \delta M(i\Delta) - 0.07685\ \delta\theta(i\Delta)$$

$$- 0.006603\ \delta\dot{\theta}(i\Delta) - 0.009451\ \delta\theta[(i-4)\Delta]$$

$$- 0.01989\ \delta\theta[(i-3)\Delta] - 0.02093\ \delta\theta[(i-2)\Delta]$$

$$- 0.02202\ \delta\theta[(i-1)\Delta] \tag{48}$$

For A, B, and x as given in equations (34), (35), and (36), the optimal regulator procedure gave the control law

$$\delta\dot{\theta}_A(i\Delta) = 27.31\ \delta M(i\Delta) - 0.06776\ \delta\theta(i\Delta)$$

$$- 0.006142\ \delta\dot{\theta}(i\Delta) - 0.6808\ \delta\theta_A(i\Delta)$$

$$- 0.008148\ \delta\theta[(i-4)\Delta] - 0.01712\ \delta\theta[(i-3)\Delta]$$

$$- 0.01801\ \delta\theta[(i-2)\Delta] - 0.01895\ \delta\theta[(i-1)\Delta] \tag{49}$$

In the eigenvalue placement algorithm (refs. 3 and 4), the designer selects the eigenvalues of $(A - Bf')$ which in turn determines the speed of closed-loop response. It was generally found that significant improvement in the Mach number response speed could not be obtained using control law (8) and the eigenvalue placement algorithm without violating constraints (37) and (38). Results are therefore only presented for eigenvalue placement using the actuator rate input (eq. (9)). The eigenvalues of A given by equation (34) are as follows:

Eigenvalue	Mode
0.950	Mach number
1.0	Integrator
$0.579 \pm j(0.218)$	Actuator
0	
0	
0	Delayed states
0	

14

The delayed states are in deadbeat form and need no alteration. The actuator dynamics cannot be physically altered. Only the Mach number and integrator modes are available for design. The best results were obtained when f was selected to cause both these eigenvalues to take on the value 0.9. The resulting control law is

$$\delta\dot{\theta}_A(i\Delta) = 31.833 \; \delta M(i\Delta) - 0.0789 \; \delta\theta(i\Delta)$$

$$- 0.007218 \; \delta\dot{\theta}(i\Delta) - 1.490 \; \delta\theta_A(i\Delta)$$

$$- 0.009482 \; \delta\theta[(i - 4)\Delta] - 0.01995 \; \delta\theta[(i - 3)\Delta]$$

$$- 0.02100 \; \delta\theta[(i - 2)\Delta] - 0.02209 \; \delta\theta[(i - 1)\Delta] \tag{50}$$

In order to demonstrate the characteristics of the optimal regulator and eigenvalue placement control laws, the transient response from a steady-state condition at Mach 0.8 is calculated. Initially,

$$\delta M(0) = M(0) - M_f$$

$$= 0.8 - 0.9$$

$$= -0.1 \tag{51}$$

Moreover, the steady-state condition implies that, for $t \leqq 0$,

$$\left.\begin{array}{l} \delta M(t) \equiv -0.1 \\ \delta\dot{\theta}(t) \equiv 0 \\ \delta\theta_A(t) \equiv \delta\theta(t) \end{array}\right\} \tag{52}$$

Then, from equation (31) or equation (34), it can be seen that

$$\delta M[(i + 1)\Delta] = 0.95035 \; \delta M(i\Delta) - 0.0002831 \; \delta\theta[(i - 4)\Delta]$$

$$- 0.0002979 \; \delta\theta[(i - 3)\Delta] \tag{53}$$

Substituting

$$\delta\theta[(i - 4)\Delta] = \delta\theta[(i - 3)\Delta] = \delta\theta(t)$$

15

and

$$\delta M \left[(i + 1) \Delta \right] = \delta M (i \Delta) = -0.1$$

into equation (53) gives

$$\delta \theta(t) = 8.55^{\circ} \tag{54}$$

for $t \leqq 0$.

The open-loop Mach number and guide vane angle responses to initial conditions of equations (51) and (52) using control inputs

$$\delta \theta_A(t) = \theta_A(t) - \theta_f \equiv 0 \tag{55}$$

are shown in figure 4. There it is shown that the variational Mach number dynamics, linearized about $M_f = 0.9$, is self-regulating; that is, $\delta M(t)$ converges monotonically without overshoot to the origin ($M = 0.9$) with no $\delta \theta_A$ input. Since the eigenvalues of equation (31) are within the unit circle of the complex plane, self-regulation occurs for all initial conditions $\delta M(0)$. Convergence to 0.9 is assumed to have occurred when a settling time t_s is reached such that

$$\left| \delta M(t) \right| \leqq 0.002 \quad \text{for} \quad t \geqq t_s \tag{56}$$

For figure 4, settling time t_s is 8.4 sec.

Figure 5 shows the closed-loop Mach number and guide vane angle responses with the optimal regulator actuator position input control law (48). The Mach number response monotonically increases to M_f with a settling time of 5.7 sec or an improvement of 2.7 sec over the open-loop results. Guide vane action is smooth with a steady-state value of $\theta_f = 1.93^{\circ}$. The guide vane angle initially decreases in order to increase Mach number.

Figure 6 shows the responses with the optimal regulator actuator rate input control law (49). Mach number convergence is no longer monotonic. Overshoot ($M > 0.9$) occurs at about 5.4 sec and does not settle down to within ±0.002 until 7.4 sec. Guide vane angle convergence to θ_f is slower than that shown in figure 4.

The responses with the eigenvalue placement actuator rate input control law (50) are shown in figure 7. Mach number convergence is monotonic with no overshoot. The settling time is about 6.3 sec.

Based on the linear simulation, control law (48) has the better performance – monotonic behavior with lower settling time. Control law (49) controls only slightly better than the open-loop response. The overshoot causes a time-consuming delay in convergence. Control law (50) has excellent characteristics but a longer settling time than control law (48). However, control law (50) is found to perform better than control law (48) when tested on the more realistic nonlinear simulation described in the next section.

<div align="center">NONLINEAR SIMULATION</div>

The physics of actual fluid flow in the NTF produce interactions between the temperature, pressure, and Mach number control loops which were not accounted for in the previous linear simulation. In order to test control laws (48) to (50) in a more realistic situation, they are applied to a one-dimensional distributed parameter model of the NTF which is based on the Navier-Stokes equations for unsteady flow. Control laws developed by Gumas for temperature and pressure regulation are employed in this nonlinear simulation to maintain total temperature and total pressure at steady flow values during Mach number transitions effected by control laws (48) to (50). The performance of these control laws when applied to the distributed parameter model is compared to that observed using the linear model.

The distributed parameter model of the NTF is realized by solving the Navier-Stokes partial differential equations of fluid flow (including viscous and thermal terms) by means of McCormack's predictor-corrector method and the use of an artificial viscosity technique for treating shocks. Tunnel geometry, liquid nitrogen injection, gas venting, and fan dynamics are introduced in the boundary conditions. Actuator dynamics, valve calibrations, fan-flow and thermal relationships, heat transfer of gas to tunnel liner, flow dynamics of test section to plenum, tunnel-wall flow losses, screen and turning-vane losses, strutsting drag losses, and sensor dynamics are all included in the model. The model is simulated on a vector-processing digital computer requiring approximately 11 sec of machine time for each second of simulated time.

Gumas' control laws for total pressure and temperature act independently of each other and the Mach control loop. Both control loops are of the proportional-integral (PI) form designed for both steady-state regulation and state transition control.

In the pressure control loop, total pressure is sensed in the stagnation section of the NTF and subtracted from the pressure set-point value to produce an input error signal to a PI controller. The PI controller output is summed with a feed-forward signal, which is a filtered value of the estimated vent-valve position necessary to achieve the commanded pressure set point. This forms the position command to the vent-valve actuator. Vent flow then establishes total pressure.

The temperature control loop is somewhat more complex. In the regulation mode, total temperature, also sensed in the NTF stagnation section, is sub-

tracted from a fixed-temperature set-point value, and the error is input to a PI controller. The PI controller output is combined with fan operating parameters in a predictive control law which estimates the LN_2 flow rate necessary to maintain an energy balance in the tunnel. The estimated LN_2 flow rate, after passing through a lead-lag network which compensates for temperature sensor time lags, is input to an LN_2 valve control loop. This loop establishes the valve position needed to produce the required LN_2 flow rate. This maintains the total temperature. During transition control, the PI controller is inactive to prevent reset windup, and a slowly varying temperature set point, programmed to assure a smooth temperature change, is furnished to the predictive control law. The transition control mode was not employed in the tests reported herein.

Figure 8 shows the open-loop Mach number and guide vane angle responses of the distributed parameter model, which corresponds to the linear case shown in figure 4. Note that the initial value for $\theta(0)$ in figure 8 differs from the value in figure 4. This is because the value in figure 8 is the actual steady-state value at Mach 0.8 for the distributed model, whereas the value for figure 4 is the predicted value from the linear equations. Figures 9, 10, and 11 show Mach number and guide vane angle responses of the distributed parameter model for optimal regulator control laws (48), (49) and the eigenvalue placement control law (50), respectively. The results are seen to be similar to the linear cases shown in figures 5 to 7. Control law (50) gives the smoothest and most rapid performance of the three cases shown. A comparison of settling times for the linear and nonlinear cases for open-loop and control laws (48) to (50) is presented in table IV.

CONCLUDING REMARKS

A transfer function for the Mach number to guide vane angle control loop has been employed to demonstrate the application of multivariable design methods to the control of the National Transonic Facility (NTF). For a typical NTF operating point, digital forms of the optimal linear regulator and eigenvalue techniques were applied to produce zero-order hold control laws for the guide-vane actuator and actuator rate inputs. When evaluated in a realistic simulation of the NTF process, the optimal regulator actuator input control laws and eigenvalue placement actuator rate input control laws reduced the settling time for an open-loop input by more than 27 percent. However, the control law derived from eigenvalue placement theory gave a preferable Mach number response. Given a transfer matrix (relating, for example, total temperature, total pressure, Mach number to injection rate, vent rate, guide vane angle), the procedure described in this paper could be applied to produce digital control laws which would regulate the state variables about a given design point and account for cross-coupling between the modes.

Langley Research Center
National Aeronautics and Space Administration
Hampton, VA 23665
June 23, 1981

18

APPENDIX

APPROXIMATION OF TIME-DELAY ORDINARY DIFFERENTIAL SYSTEMS BY

FINITE-DIFFERENCE EQUATIONS

Given a time invariant system with state $x(t)$, control $u(t)$, and a delay $h > 0$ such that

$$\tilde{x}(t) = \tilde{x}_o(t), \quad u(t) = u_o(t) \quad \text{for} \quad -h \leqq t \leqq 0$$

where the subscript o denotes initial condition and

$$\frac{d}{dt} \tilde{x}(t) = A_0 \tilde{x}(t) + A_1 \tilde{x}(t - h) + B_0 u(t) + B_1 u(t - h) \tag{A1}$$

for $0 \leqq t \leqq T$, a method is presented for approximating equation (A1) by the finite-difference equation

$$\tilde{x}[(i + 1)\Delta] = \hat{A}_0 \tilde{x}(i\Delta) + \hat{A}_1 \tilde{x}[(i - m)\Delta] + \hat{A}_2 \tilde{x}[(i - m + 1)\Delta]$$

$$+ \hat{B}_0 u(i\Delta) + \hat{B}_1 u[(i - m)\Delta] \qquad (i = 0,1,\ldots,N; \quad N\Delta = T) \tag{A2}$$

In equation (A2), $\hat{A}_0$, $\hat{A}_1$, $\hat{A}_2$, $\hat{B}_0$, and $\hat{B}_1$ are constant matrices, the control $u(t)$ has been assumed to have zero-order hold structure with sampling period Δ, and m is a nonnegative integer chosen such that $m\Delta$ approximates the time delay h. Using equation (A2) and a new state vector generally structured as

$$x(i\Delta) = \text{col}\{\tilde{x}(i\Delta), \tilde{x}[(i - 1)\Delta], \tilde{x}[(i - 2)\Delta],\ldots,\tilde{x}[(i - m)\Delta],$$

$$u[(i - 1)\Delta], u[(i - 2)\Delta],\ldots,u[(i - m)\Delta]\} \tag{A3}$$

the system dynamics can be stated in the form

$$x[(i + 1)\Delta] = A x(i\Delta) + B u(i\Delta) \qquad (i = 0,1,\ldots,N) \tag{A4}$$

to which modern control theory can be readily applied.

APPENDIX

Begin by partitioning the interval $[0,T]$ into segments t_i, $(i = 0,1,\ldots,N)$ such that

$$0 = t_0 < t_1 < t_2 < \ldots < t_{N-1} < t_N = T \tag{A5}$$

The solution of equation (A1) at points t_i is

$$\tilde{x}(t_{i+1}) = e^{A_0(t_{i+1}-t_i)}\,\tilde{x}(t_i) + \int_{t_i}^{t_{i+1}} e^{A_0(t_{i+1}-\tau)}\,A_1\,x(\tau - h)\,d\tau$$

$$+ \int_{t_i}^{t_{i+1}} e^{A_0(t_{i+1}-\tau)}\,B_0\,u(\tau)\,d\tau$$

$$+ \int_{t_i}^{t_{i+1}} e^{A_0(t_{i+1}-\tau)}\,B_1\,u(\tau - h)\,d\tau \tag{A6}$$

or, if $\Delta_i = t_{i+1} - t_i$,

$$\tilde{x}(t_{i+1}) = e^{A_0\Delta_i}\,\tilde{x}(t_i) + \int_0^{\Delta_i} e^{A_0\tau}\,A_1\,\tilde{x}(t_{i+1} - \tau - h)\,d\tau$$

$$+ \int_0^{\Delta_i} e^{A_0\tau}\,B_0\,u(t_{i+1} - \tau)\,d\tau$$

$$+ \int_0^{\Delta_i} e^{A_0\tau}\,B_1\,u(t_{i+1} - \tau - h)\,d\tau \tag{A7}$$

Let $t_i = i\Delta$ with Δ constant and assume

$$h \approx m\Delta \tag{A8}$$

whereby equation (A7) becomes

$$\tilde{x}[(i + 1)\Delta] = e^{A_0\Delta} \tilde{x}(i\Delta) + \int_0^\Delta e^{A_0\tau} A_1 \tilde{x}[(\Delta - \tau) + (i - m)\Delta] d\tau$$

$$+ \int_0^\Delta e^{A_0\tau} B_0 u[(i + 1)\Delta - \tau] d\tau$$

$$+ \int_0^\Delta e^{A_0\tau} B_1 u[(\Delta - \tau) + (i - m)\Delta] d\tau \qquad (A9)$$

Next impose a zero-order hold form for the control function $u(t)$ such that

$$u(t) = u(i\Delta) = \text{Constant}, \quad t\epsilon[i\Delta, (i + 1)\Delta) \qquad (i = 0, 1, \ldots, N - 1) \qquad (A10)$$

Substituting equation (A10) into equation (A9) gives

$$\tilde{x}[(i + 1)\Delta] = \left[e^{A_0\Delta}\right] \tilde{x}(i\Delta) + \int_0^\Delta e^{A_0\tau} A_1 \tilde{x}[(\Delta - \tau) + (i - m)\Delta] d\tau$$

$$+ \left[\int_0^\Delta e^{A_0\tau} B_0 d\tau\right] u(i\Delta) + \left[\int_0^\Delta e^{A_0\tau} B_1 d\tau\right] u[(i - m)\Delta] \qquad (A11)$$

Finally, applying the trapezoidal integration rule to approximate the first integral in equation (A11)

$$\int_0^\Delta e^{A_0\tau} A_1 \tilde{x}[(\Delta - \tau) + (i - m)\Delta] d\tau$$

$$\approx \left[\frac{\Delta}{2} e^{A_0\Delta} A_1\right] \tilde{x}[(i - m)\Delta] + \left[\frac{\Delta}{2} A_1\right] \tilde{x}[(i + 1 - m)\Delta]$$

$$(A12)$$

equation (A11) appears in the form of equation (A2) with

$$\hat{A}_0 = e^{A_0 \Delta}$$

$$\hat{A}_1 = \frac{\Delta}{2} e^{A_0 \Delta} A_1$$

$$\hat{A}_2 = \frac{\Delta}{2} A_1$$

$$\hat{B}_0 = \int_0^{\Delta} e^{A_0 \tau} \, d\tau \, B_0$$

$$\hat{B}_1 = \int_0^{\Delta} e^{A_0 \tau} \, d\tau \, B_1$$

$$(A13)$$

REFERENCES

1. McKinney, Linwood W.; and Howell, Robert R.: The Characteristics of the
   Planned National Transonic Facility. Proceedings - AIAA 9th Aerodynamic
   Testing Conference, June 1976, pp. 176-184.

2. Gumas, George: The Dynamic Modelling of a Slotted Test Section.
   NASA CR-159069, 1979.

3. Armstrong, Ernest S.: ORACLS - A Design System for Linear Multivariable
   Control. Marcel Dekker, Inc., c.1980.

4. Kwakernaak, Huibert; and Sivan, Raphael: Linear Optimal Control Systems.
   John Wiley & Sons, Inc., c.1972.

TABLE I.- VALUES OF TIME CONSTANT τ AND GAIN k

FOR $T_{t,f} = 111.11$ K $(-260^{\circ}F)$

M_f	rpm	τ, sec	k, deg^{-1}
0.4	160	1.17	-0.00344
.5	160	1.15	-.00435
.6	240	1.69	-.00734
.7	240	2.08	-.00834
.8	240	2.39	-.00978
.9	360	2.58	-.01415
1.0	360	2.76	-.0144
1.1	360	1.97	-.0102
1.2	360	1.69	-.00836

TABLE II.- VALUES OF TIME CONSTANT τ AND GAIN k

FOR $T_{t,f} = 166.67$ K $(-160^{\circ}F)$

M_f	rpm	τ, sec	k, deg^{-1}
0.4	200	0.980	-0.00364
.5	240	1.068	-.00477
.6	240	1.228	-.00573
.7	360	1.640	-.01089
.8	360	1.968	-.0119
.9	360	1.964	-.0117
1.0	360	2.020	-.0124
1.1	360	1.1418	-.00965

TABLE III.- VALUES OF TIME CONSTANT τ AND GAIN k

FOR $T_{t,f} = 222.22$ K (-60° F)

M_f	rpm	τ, sec	k, deg^{-1}
0.4	240	0.739	-0.00290
.5	240	.830	-.00403
.6	360	1.150	-.00820
.7	360	1.470	-.00920
.8	360	1.640	-.01010
.9	360	1.690	-.01110
1.0	360	1.760	-.01330

TABLE IV.- MACH NUMBER SETTLING TIMES FOR LINEAR

AND NONLINEAR SIMULATIONS

Control law	Settling times, sec $\|\delta M\| \leqq 0.002$	
	Linear	Nonlinear
$\theta_A(t) \equiv \theta_f$	8.4	5.5
Equation (48)	5.7	4.0
Equation (49)	7.4	7.0
Equation (50)	6.3	4.0
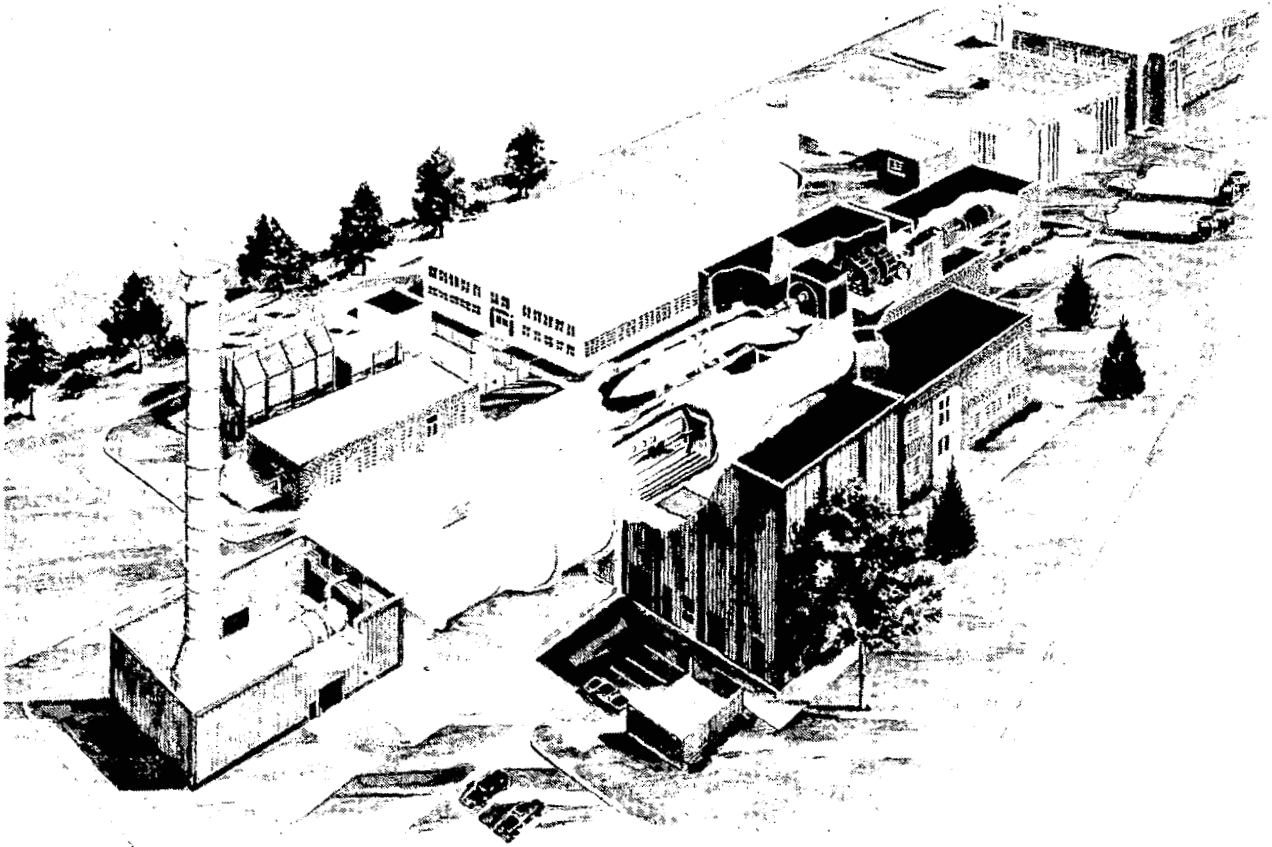
Figure 1.- National Transonic Facility.

L-78-503
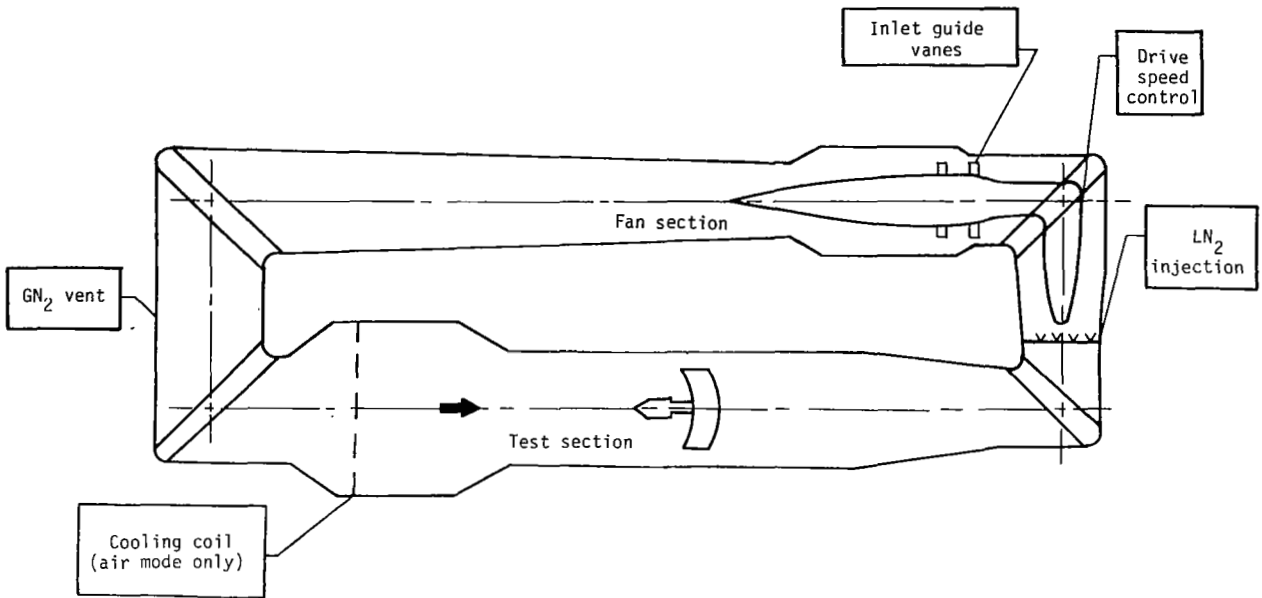
Figure 2.- NTF control element locations.
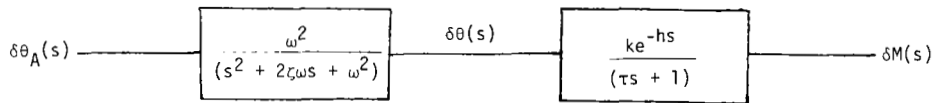
(a) $\delta\theta_A$ as control.
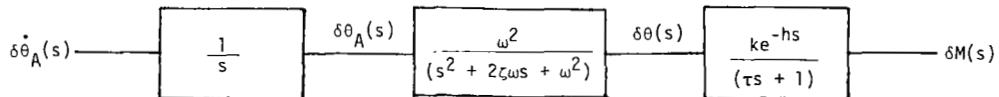
(b) $\delta\dot{\theta}_A$ as control.

Figure 3.- Block diagrams for NTF Mach number control loop.
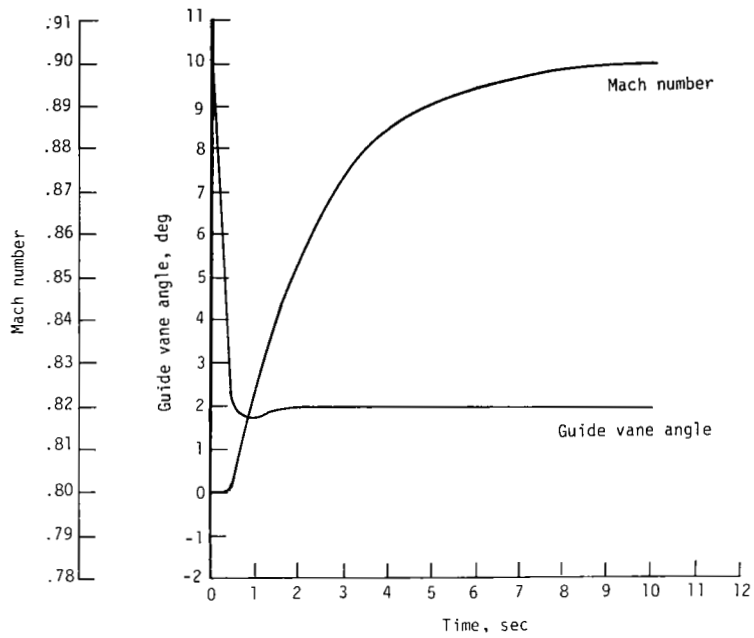
Figure 4.- Open-loop response - linear simulation.
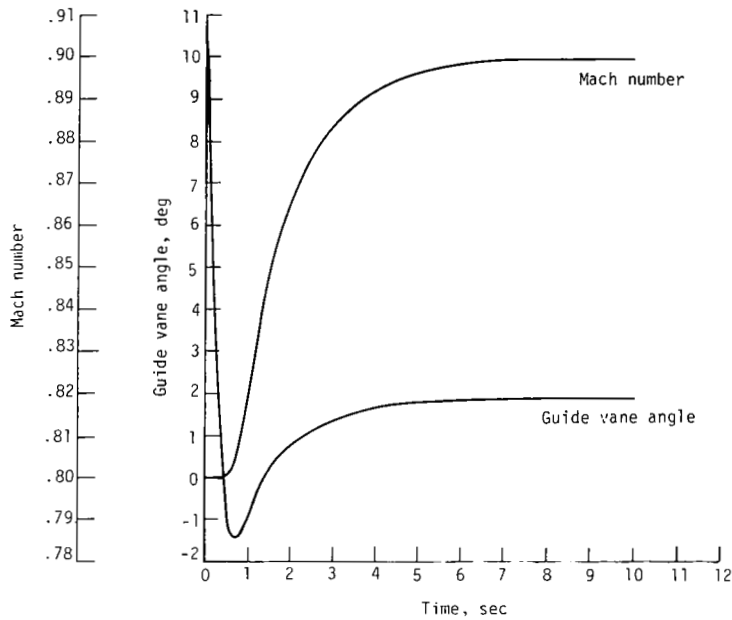
Figure 5.- Optimal regulator for actuator rate input control law (48) -
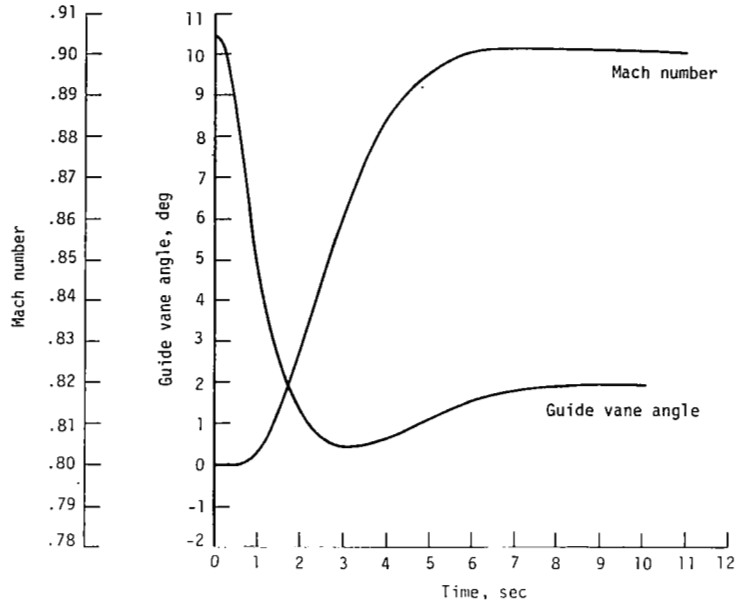linear simulation.

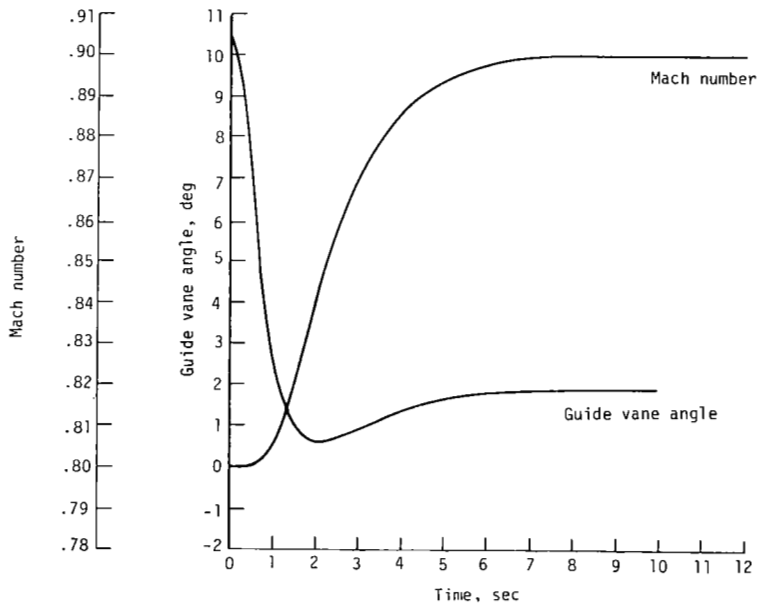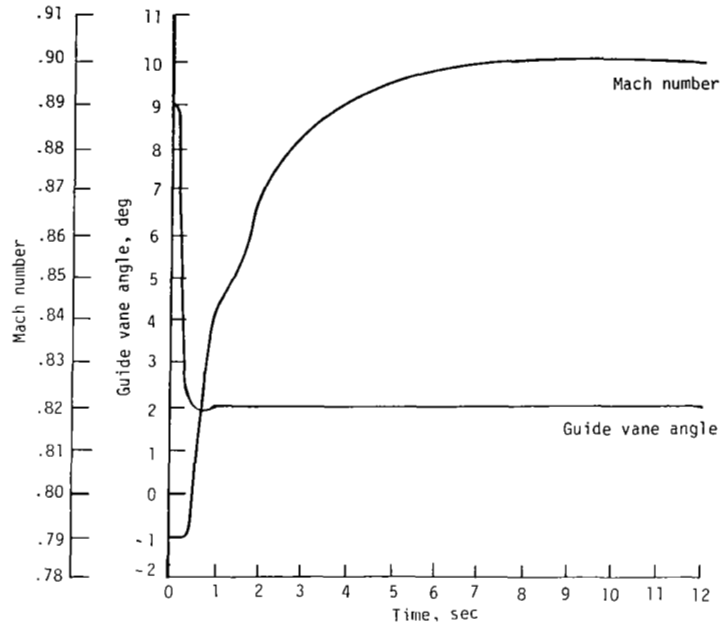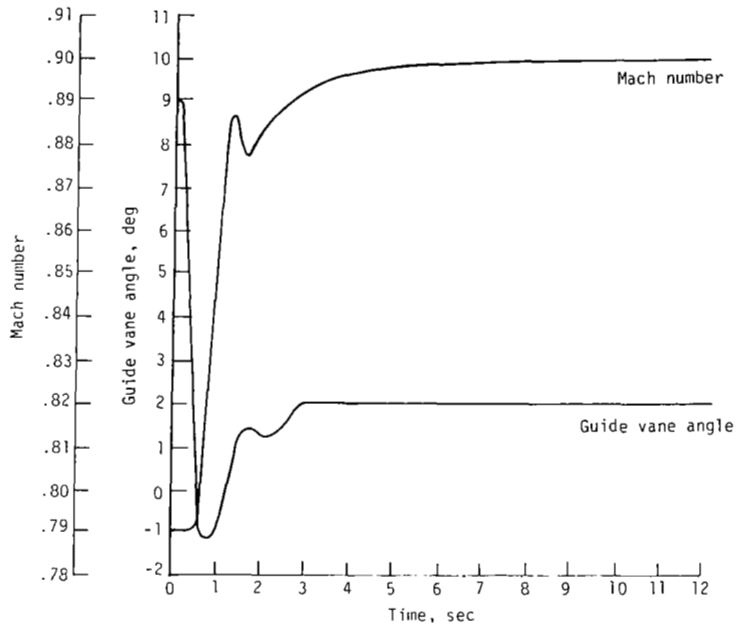Figure 6.- Optimal regulator for actuator rate input control law (49) -
linear simulation.

Figure 7.- Eigenvalue placement for actuator rate input control law (50) -
linear simulation.

29

Figure 8.- Open-loop response - nonlinear simulation.

Figure 9.- Optimal regulator for actuator input control law (48) - nonlinear simulation.
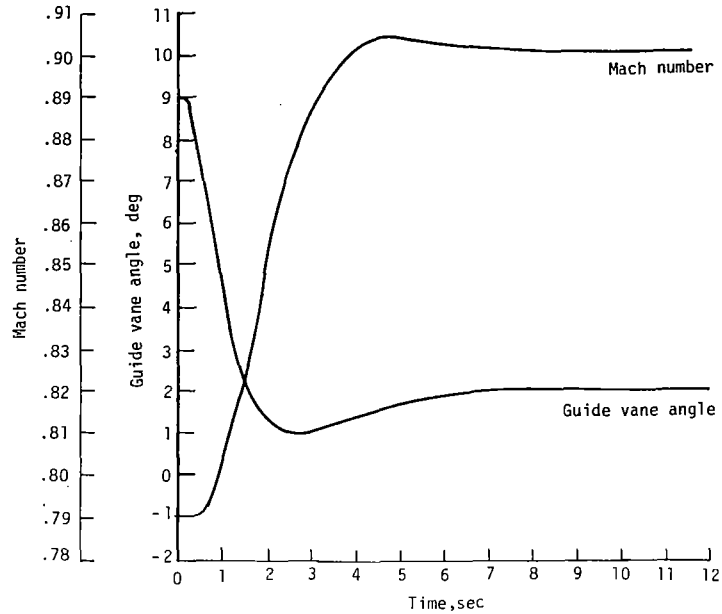
30

Figure 10.- Optimal regulator for actuator rate input control law (49) -
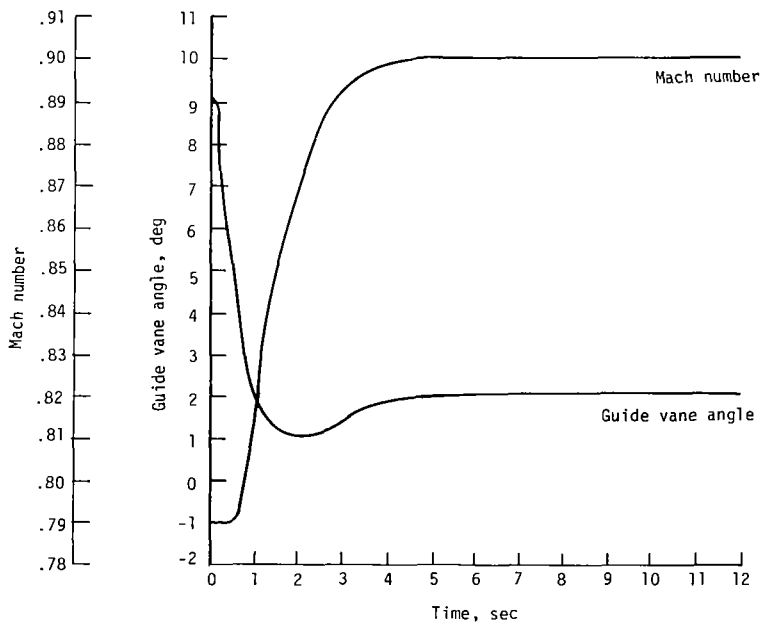nonlinear simulation.

Figure 11.- Eigenvalue placement for actuator rate input control law (50) -
nonlinear simulation.

1. Report No. NASA TP-1887	2. Government Accession No.	3. Recipient's Catalog No.
4. Title and Subtitle AN APPLICATION OF MULTIVARIABLE DESIGN TECHNIQUES TO THE CONTROL OF THE NATIONAL TRANSONIC FACILITY		5. Report Date August 1981
		6. Performing Organization Code 505-34-33-02
7. Author(s) Ernest S. Armstrong and John S. Tripp		8. Performing Organization Report No. L-14491
		10. Work Unit No.
9. Performing Organization Name and Address NASA Langley Research Center Hampton, VA 23665		11. Contract or Grant No.
		13. Type of Report and Period Covered Technical Paper
12. Sponsoring Agency Name and Address National Aeronautics and Space Administration Washington, DC 20546		14. Sponsoring Agency Code

15. Supplementary Notes

16. Abstract

The digital versions of optimal-linear-regulator theory and eigenvalue placement theory are applied to the Mach number control loop of the National Transonic Facility cryogenic wind tunnel. The control laws developed are evaluated on a nonlinear simulation of the tunnel process for a typical test condition and are found to significantly reduce the open-loop time required to achieve a Mach number set point.

17. Key Words (Suggested by Author(s)) Multivariable feedback control Optimal control Process control Wind tunnels Digital techniques	18. Distribution Statement Unclassified - Unlimited Subject Category 63

19. Security Classif. (of this report) Unclassified	20. Security Classif. (of this page) Unclassified	21. No. of Pages 32	22. Price A03

National Aeronautics and
Space Administration

Washington, D.C.
20546

THIRD-CLASS BULK RATE

U.S.MAIL

```
  8    1 1U,G,         080481 S00903DS
DEPT OF THE AIR FORCE
AF WEAPONS LABORATORY
ATTN: TECHNICAL LIBRARY (SUL)
KIRTLAND AFB NM 87117
```

NASA